

## RESEARCH

# NETest liquid biopsy is diagnostic of small intestine and pancreatic neuroendocrine tumors and correlates with imaging

Anna Malczewska<sup>1</sup>, Magdalena Witkowska<sup>1</sup>, Karolina Makulik<sup>1</sup>, Agnes Bocian<sup>1</sup>, Agata Walter<sup>1</sup>, Joanna Pilch-Kowalczyk<sup>2</sup>, Wojciech Zajęcki<sup>3</sup>, Lisa Bodei<sup>4</sup>, Kjell Oberg<sup>5</sup> and Beata Kos-Kudła<sup>1</sup>

<sup>1</sup>Department of Endocrinology and Neuroendocrine Tumors, Department of Pathophysiology and Endocrinology, Medical University of Silesia, Katowice, Poland

<sup>2</sup>Department of Radiology and Nuclear Medicine, Medical University of Silesia, Katowice, Poland

<sup>3</sup>Department of Pathology in Zabrze, Medical University of Silesia, Katowice, Poland

<sup>4</sup>Molecular Imaging and Therapy Service, Department of Radiology, Memorial Sloan Kettering Cancer Center, New York, New York, USA

<sup>5</sup>Department of Endocrine Oncology, University Hospital, Uppsala, Sweden

Correspondence should be addressed to A Malczewska or K Oberg: [malczewska.an@gmail.com](mailto:malczewska.an@gmail.com) or [kjell.oberg@medsci.uu.se](mailto:kjell.oberg@medsci.uu.se)

## Abstract

**Introduction:** Current monoanalyte biomarkers are ineffective in gastroenteropancreatic neuroendocrine tumors (GEP-NETs). NETest, a novel multianalyte signature, provides molecular information relevant to disease biology.

**Aim(s):** Independently validate NETest to diagnose GEP-NETs and identify progression in a tertiary referral center.

**Materials and methods:** Cohorts are 67 pancreatic NETs (PNETs), 44 small intestine NETs (SINETs) and 63 controls. Well-differentiated (WD) PNETs,  $n = 62$ , SINETs, all ( $n = 44$ ). Disease extent assessment at blood draw: anatomical ( $n = 110$ ) CT ( $n = 106$ ), MRI ( $n = 7$ ) and/or functional <sup>68</sup>Ga-SSA-PET/CT ( $n = 69$ ) or <sup>18</sup>F-FDG-PET/CT ( $n = 8$ ). Image-positive disease (IPD) was defined as either CT/MRI or <sup>68</sup>Ga-SSA-PET/CT/<sup>18</sup>F-FDG-PET/CT-positive. Both CT/MRI and <sup>68</sup>Ga-SSA-PET/CT negative diagnosis in WD-NETs was considered image-negative disease (IND). NETest (normal: 20); PCR (spotted plates). Data: mean  $\pm$  SD.

**Results:** Diagnosis: NETest was significantly increased in NETs ( $n = 111$ ;  $26 \pm 21$ ) vs controls ( $8 \pm 4$ ,  $p < 0.0001$ ). Seventy-five (42 PNET, 33 SINET) were image positive. Eleven (8 PNET, 3 SINET; all WD) were IND. In IPD, NETest was significantly higher ( $36 \pm 22$ ) vs IND ( $8 \pm 7$ ,  $P < 0.0001$ ). NETest accuracy, sensitivity and specificity are 97, 99 and 95%, respectively. Concordance with imaging: NETest was 92% (101/110) concordant with anatomical imaging, 94% (65/69) with <sup>68</sup>Ga-SSA-PET/CT and 96% (65/68) dual modality (CT/MRI and <sup>68</sup>Ga-SSA-PET/CT). In 70 CT/MRI positive, NETest was elevated in all ( $37 \pm 22$ ). In 40 CT/MRI negative, NETest was normal ( $11 \pm 10$ ) in 31. In 56 <sup>68</sup>Ga-SSA-PET/CT positive, NETest was elevated ( $36 \pm 22$ ) in 55. In 13 <sup>68</sup>Ga-SSA-PET/CT negative, NETest was normal ( $9 \pm 8$ ) in ten. Disease status: NETest was significantly higher in progressive ( $61 \pm 26$ ;  $n = 11$ ) vs stable disease ( $29 \pm 14$ ;  $n = 64$ ;  $P < 0.0001$ ) (RECIST 1.1).

**Conclusion:** NETest is an effective diagnostic for PNETs and SINETs. Elevated NETest is as effective as imaging in diagnosis and accurately identifies progression.

## Key Words

- ▶ NETest
- ▶ liquid biopsy
- ▶ biomarker
- ▶ gastroenteropancreatic
- ▶ imaging

Endocrine Connections  
(2019) 8, 442–453

## Introduction

Neuroendocrine tumors (NETs) have increased in incidence with small intestine NETs (SINETs) being the most common and pancreatic NETs (PNETs), the third most common among gastroenteropancreatic (GEP) NETs per the SEER database (1). The increase has been attributed *inter alia* to improvements in tumor detection. However, current diagnostic strategies that depend on suspicious symptomatology are ineffective as 40–50% of SINETs and PNETs are not detected until distant metastases develop (2); this significantly worsens prognosis (3). The majority of PNETs (60–90%) are non-functional and, in general, are diagnosed at a more advanced disease stage than functional (F) tumors due to the absence of ‘alarming’ symptoms (4). The most common F-PNETs are insulinomas. These are principally benign (>90%) and only ~10% represent a diagnostic and therapeutic challenge (4, 5). SINETs are not usually clinically symptomatically active until hepatic metastasis (30–40%) (6). In PNETs without liver involvement, carcinoid syndrome occurs very rarely (2). Circulating indicators of tumor secretory functionality (amines or peptides) hence represent a minority of NETs. Measurement of secretory biomarkers is therefore *de facto* clinically limited. Chromogranin A (CgA), previously considered the neuroendocrine pan-biomarker, reflects secretory activity rather than tumor biology, heterogeneity or plasticity (7, 8). It has limited clinical utility as well as methodological restrictions (9, 10).

Imaging remains a key component of diagnostic work-up or disease monitoring, for example, identification of disease status or therapeutic efficacy (11). RECIST and RECIST 1.1 criteria, most-widely used for the assessment of response in clinical trials, were developed based on data from testing cytotoxic drugs (12). It exhibits limitations in indolent NETs (13, 14) and has issues with the assessment of disease stabilization and ‘pseudo-progression’ (related to targeted therapy), reproducibility, lesion dimensionality evaluation or accurate delineation of metastatic disease, in particular in the extra-hepatic location. Functional molecular imaging with somatostatin receptor-based strategies for example, <sup>68</sup>Ga-SSA-PET/CT, has improved the sensitivity of NET detection (15), especially in extra-hepatic localization. It has benefit in the assessment of eligibility for peptide receptor radionuclide therapy (PRRT) and somatostatin analogs (SSAs). Its accuracy, however, is limited by resolution (~5–8 mm for PET scanners), volume averaging of small lesions with adjacent normal tissues with resulting normal/low uptake, elevated background liver uptake, tumor heterogeneity or somatostatin

receptor (SSTR) status and so forth. No imaging modality is exclusively effective and all are expensive and all except MRI involve radiation. The combination of anatomic and functional modalities is effective in amplifying sensitivity and specificity parameters for detection (13); this, however, increases radiation exposure.

A concern with imaging accuracy has been identified by pathological examination of liver resections from SINETs and PNETs which reveals that in >50% (more in SINETs than PNETs), micrometastases is not detectable by various imaging modalities or macroscopic gross examination (16, 17). The incidence of occult or covert disease, especially in the liver, is therefore likely significantly higher than reported (17) and, in consequence, disease burden is underestimated. While metastatic disease represents a significant negative prognostic factor (3, 18), a key issue in GEP-NET management is the early identification of progressive disease at the initial stages of the metastatic cascade. As a result, there can be a time delay in the introduction of efficacious treatment. To date, no blood-based biomarker for prediction of treatment efficacy is available except the positive predictor quotient for PRRT (19).

Emerging precision medicine strategies have drawn attention to the utilization of molecular tools such as non-invasive liquid biopsies (circulating biomarkers) to facilitate and optimize cancer management in many cancers (20). Recently, a molecular NET transcriptomic analysis (NETest) has been proposed as a NET liquid biopsy (21). The NETest, as opposed to CgA or other monoanalyte peptides/hormones, is a multianalyte molecular signature representing biological information pertinent to the clinical neuroendocrine disease course. It has numerous documented applications including diagnosis, identification of residual disease post surgery, disease status identification and assessment of treatment efficacy (22). The NETest has been shown to correlate with disease positivity on imaging (23). In addition, a positive blood result can also precede the standard imaging detection of the disease by 1–2 years (24). Independent validation of this NET liquid biopsy is required. We therefore undertook to validate the NETest as a diagnostic and disease status identification marker in SINETs and PNETs under real-world conditions.

## Aims

The current study independently assessed the diagnostic accuracy of the NETest in SINET and PNET and for identification of progressive versus stable disease in a

tertiary referral center. We compared NETest results to controls, assessed the concordance between NETest levels and imaging (anatomical/functional) at the time of blood draw and evaluated its accuracy for the delineation of disease status (stable and progressive disease) as defined by RECIST 1.1.

## Materials and methods

### Strategy

We examined circulating NETest levels from PNETs ( $n=67$ ) and SINETs ( $n=44$ ) and compared these with controls ( $n=63$ ). The diagnostic accuracy and metrics (AUROC (area under the receiver operating characteristic curve), sensitivity, specificity) for the NETest were calculated. The concordance of the NETest levels with imaging was then assessed. Disease extent was determined at blood draw by anatomical imaging ( $n=110$ ): CT ( $n=106$ ) or MRI ( $n=7$ ) and/or functional –  $^{68}\text{Ga}$ -DOTA-TATE PET/CT ( $n=69$ ) in WD NETs or  $^{18}\text{F}$ -FDG-PET/CT ( $n=8$ ) in G2/G3 NETs (Fig. 1). Image-positive disease (IPD) was defined as either CT or MRI or  $^{68}\text{Ga}$ -SSA/ $^{18}\text{F}$ -FDG-PET/CT positive. Image-negative disease (IND) was anatomically (CT/MRI) and functionally  $^{68}\text{Ga}$ -SSA-PET/CT (in WD NETs) negative.

### Imaging

For radiological assessment of the disease, anatomical and functional imaging modalities were utilized. Anatomical imaging comprised multiphase CT with administration of iodine contrast (in two cases, CT without contrast was performed: one due to renal failure and the second due to contrast allergy). Most were performed by the 16-slice LightSpeed CT Scanner (General Electrics, Boston, MA, USA) (the slice thickness was 1.25 and 2.5 mm for the examination of the pancreas and 2.5 mm for the bowel) or multiphase MRI. The latter were performed using the 1.5T MRI scanner (General Electrics) with injection of

the gadolinium contrast (slice thickness 4–6 mm), and T1/T2 sequences were obtained. The functional imaging was performed by the hybrid PET/CT scanners (positron emission tomography combined with a computer tomography scanner) with administration of  $^{68}\text{Ga}$ -DOTA-TATE in the WD NETs or  $^{18}\text{F}$ -FDG in higher grade (well- and poorly differentiated) tumors.

### Disease status

Progressive disease was defined based on anatomical imaging and RECIST 1.1 criteria. Parameters were at least 20% increase in the sum of diameters of the target lesions (min. 5 mm) measured on anatomical imaging (mostly CT) or detection of new lesions by imaging of the same modality when subsequently performed. The time interval of follow-up was a median of 8 months (range: 1.5–24 months).

### Cohorts

The study was approved by the Ethics Committee of the Medical University of Silesia. Informed written consent was obtained from all study subjects. Blood samples were collected prospectively between April 2017 and April 2018. Control subjects ( $n=63$ ) included family members of the hospital personnel, and non-affected family members of the patients attending the Endocrinology Department. Control subjects were enrolled if there was no known malignancy present at the time of blood draw and they identified themselves as asymptomatic and in good health. All NETs were histologically confirmed, with no other synchronous malignancy at blood draw. Patient cohorts included PNETs ( $n=67$ ) and SINETs ( $n=44$ ).

Sixty-five PNETs were sporadic, 2 MEN-1 related, 58 were non-functional (NF), while the 9 functional included 5 insulinomas and 4 subjects with carcinoid syndrome (CS). WD PNETs comprised 62/67 (in two no data). Grade: G1: 33, G2: 27, G3: 5.

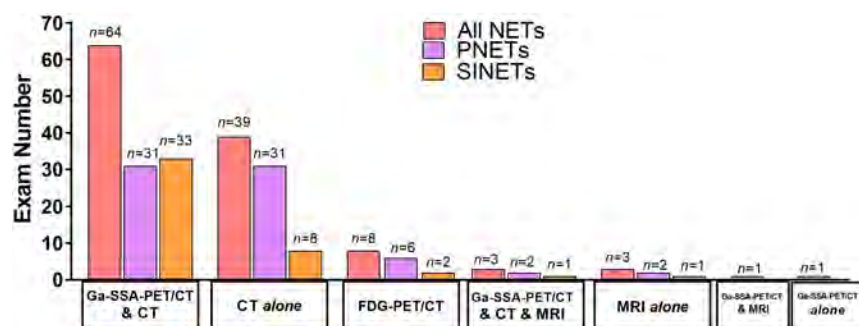


**Figure 1**

Summary of imaging modalities utilized in NETs, PNETs and SINETs. Anatomical imaging was performed in 110 NETs; functional:  $^{68}\text{Ga}$ -SSA-PET/CT in 69 and  $^{18}\text{F}$ -FDG-PET/CT in 8. Dual modality imaging:  $^{68}\text{Ga}$ -SSA-PET/CT and CT/MRI was performed in 68 NETs. All NETs: red; PNETs: purple; SINETs: orange.

**Table 1** Structure and clinicopathological data on the study cohort.

Variables	PNET	SINET	Controls
Number	67	44	63
Gender			
Males	24	26	20
Females	43	18	43
Age			
Mean (range)	56 (19–87)	59 (27–77)	44 (23–78)
Functionality status			
Non-functional	58	37	N/A
Functional	9	7	
Grade			
Grade 1	33	33	N/A
Grade 2	27	10	
Grade 3 NET	2	1	
Grade 3 NEC	3	-	
No data	2	-	
TNM stage			
Stage I	21	2	N/A
Stage IIA	8	-	
Stage IIB	4	-	
Stage IIIA	1	-	
Stage IIIB	10	16	
Stage IV	23	26	
Image-positive disease			
No.	42	33	
Stage I	10	-	N/A
Stage IIA	1	-	
Stage IIIB	8	8	
Stage IV	23	25	
Image-negative (dual modality)			
Number	8	3	N/A
Disease status (RECIST 1.1)			
Stable	34	30	N/A
Progressive	8	3	
Current treatment			
SSA	27	27	N/A
Everolimus	1	3	
Sunitinib	1	-	
Previous treatments			
Primary tumor resection	44	39	N/A
Distal pancreatectomy: 32		RHC: 25	
PancD (Traverso): 6		SBR: 14	
PancD (Whipple): 2		-	
Enucleation: 3		-	
Partial pancreatectomy: 1		-	
PRRT	11	12	
Chemotherapy	6	2	
Everolimus	1	N/A	
Loco-regional (liver)	6	3	
Radiotherapy	3	N/A	

Chemotherapy, FOLFOX, or paclitaxel + cisplatin, or etoposide + cisplatin; loco-regional therapy for liver metastases, liver resection, or RFA (radiofrequency ablation), or thermal ablation; PancD, pancreaticoduodenectomy; PRRT, peptide radioisotope receptor therapy; RHC, right hemicolectomy; SBR, small bowel resection; SSA, somatostatin analog.

The majority of SINETs (37/44) were NF, seven had CS. All were WD. Grade: G1: 33, G2: 10, G3: 1 (Table 1).

At the time of blood draw: 29 PNETs were treated – SSA ( $n=27$ ), everolimus ( $n=1$ ), sunitinib ( $n=1$ ); a majority had undergone other treatments:

pancreatic resection ( $n=44$ ), chemotherapy ( $n=6$ ), everolimus ( $n=1$ ), PRRT ( $n=11$ ), loco-regional treatment for liver metastases ( $n=6$ ), radiotherapy ( $n=3$ ). At blood draw, 30 SINETs were treated: SSA ( $n=27$ ), everolimus ( $n=3$ ); a majority had undergone other treatments:

bowel resection ( $n=39$ ), chemotherapy ( $n=2$ ), PRRT ( $n=12$ ), loco-regional treatment for liver metastases ( $n=3$ ) (Table 1).

### Blood samples collection for NETest measurement

Peripheral blood samples (3mL) were collected in EDTA tubes, mixed and stored on ice. Tubes were anonymously coded and stored at  $-80^{\circ}\text{C}$  within 2h of collection per standard molecular diagnostics protocols for PCR-based studies (24). Randomly selected coded blood samples were sent de-identified to Wren Laboratories (Branford, CT, USA).

### NETest measurement

Details of the PCR methodology, mathematical analysis and validation have been published in detail, comprising a two-step protocol (RNA isolation/cDNA production and qPCR) from EDTA-collected whole blood (24, 25, 26). The assay was undertaken in a USA clinically certified laboratory (Wren Laboratories CL-0704, CLIA 07D2081388). Transcripts (mRNA) were isolated from EDTA-collected whole blood samples (mini blood kit, Qiagen) and real-time PCR was performed on pre-spotted plates. Target transcript levels are normalized and quantified versus a population control (24, 25, 26). Final results are expressed as an activity index (NETest score) from 0 to 100% (24, 25, 26). Normal score cut-off: 20.

### Statistical analysis

The required total sample size (NETs and controls, power 0.8 and  $\alpha=0.05$ ) to attain significant differences in NETest scores was calculated to be a minimum of 42 patients/subjects in each group. Intergroup analyses were undertaken using two-tailed non-parametric tests (Mann-Whitney  $U$  test). AUROC analysis was used to determine the diagnostic accuracy of the NETest (27, 28, 29). Metrics calculated included sensitivity and specificity. Prism 7.0 for Windows (GraphPad Software, [www.graphpad.com](http://www.graphpad.com)) and MedCalc Statistical Software version 16.2.1 (MedCalc Software bvba, Ostend, Belgium; <http://www.medcalc.org>; 2017) were utilized. Statistical significance was defined as a  $P$  value  $<0.05$ . Data are presented as mean  $\pm$  SD.

## Results

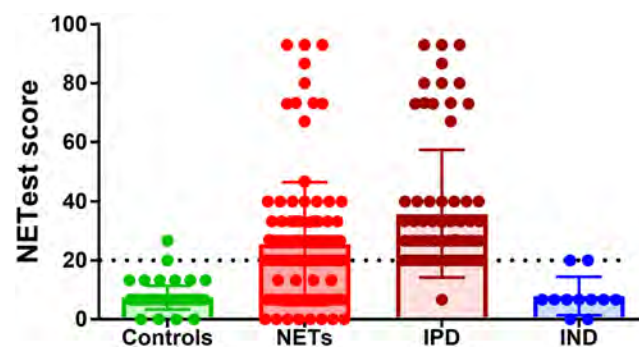
### Disease extent evaluation

Overall, IPD (any modality) was present in 75: PNETs ( $n=42$ ) – primary *in situ*/local recurrence ( $n=26$ ),

lymph node metastases ( $n=21$ ), distant metastases (liver and/or bone, other:  $n=23$ ), SINETs ( $n=33$ ): primary *in situ* ( $n=4$ ), lymph node metastases ( $n=25$ ), distant metastases (liver and/or bone, other:  $n=26$ ) (Table 1). IND was confirmed by dual (both anatomical and functional negative) imaging in 11 WD NETs (PNET:  $n=8$ ; SINET:  $n=3$ ). These were considered ‘true’ negative by imaging. Disease positive on imaging but with discordant results between anatomical and functional imaging was present in six NETs: one PNET (CT positive and  $^{68}\text{Ga}$ -SSA-PET/CT negative) and five SINETs (all CT negative and  $^{68}\text{Ga}$ -SSA-PET/CT positive).

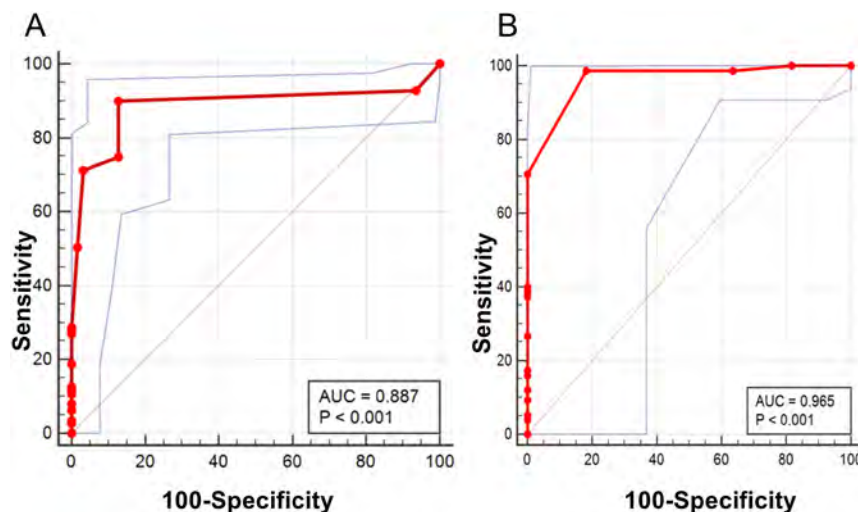
### Diagnosis

NETest levels were significantly increased ( $26 \pm 21$ ) in all GEP-NETs ( $n=111$ ) versus controls ( $8 \pm 4$ ,  $P < 0.0001$ ) (Fig. 2). NETest diagnostic metrics were accuracy (97%), sensitivity (99%) and specificity (95%). In IPD, NETest levels were  $36 \pm 22$  and in IND significantly lower ( $8 \pm 7$ ,  $P < 0.0001$ ). NETest levels in image-positive PNETs ( $37 \pm 22$ ) and SINETs ( $34 \pm 21$ ) were not different. The AUROC for differentiating all NETs (irrespective of imaging status) from controls was 0.89 (95% CI: 0.830–0.930,  $P < 0.0001$ ). The AUROC for differentiating IPD from IND was 0.96 (95% CI: 0.901–0.993,  $P < 0.0001$ ) (Fig. 3). In IPD, NETest levels were not significantly different between TNM stages or grades (Fig. 4). Eight PNETs (one stage I, seven stage IV) and three SINETs (all stage IV) were progressive by imaging (RECIST). Among these, seven NETs (four PNETs, three SINETs, all stage IV) had a high NETest score ( $79 \pm 10$ ; range 67–93%).



**Figure 2**

NETest in all NETs (SINETs and PNETs) and controls. Comparison of image-negative (IND) and image-positive NETs (IPD). The NETest measurements were elevated in the NET cohort ( $26 \pm 21$ ;  $n=111$ ) compared to controls ( $8 \pm 4$ ,  $P < 0.0001$ ;  $n=63$ ). NETest levels were elevated ( $36 \pm 22$ ) in IPD ( $n=75$ ) compared to IND ( $n=11$ ) ( $8 \pm 7$ ,  $P < 0.0001$ ). Two-tailed non-parametric tests (Mann-Whitney  $U$  test). Statistical significance was defined at a  $P$  value  $<0.05$ . Mean  $\pm$  SD.

**Figure 3**

(A) The AUROC for NETest levels in NETs and controls: The AUROC for differentiating NETs from controls was 0.89 (95% CI: 0.830–0.930,  $P < 0.0001$ ). Statistical significance was defined at a  $P$  value  $< 0.05$ . (B) The AUROC for image-positive NETs (IPD) and image-negative (IND) NETs: The AUROC for differentiating IPD from subjects who were both anatomical and functional imaging negative for disease was 0.965 (95% CI: 0.901–0.993,  $P < 0.0001$ ). Statistical significance was defined at a  $P$  value  $< 0.05$ .

### Concordance with imaging

#### PNETs

CT or MRI was performed in 66, 42 were positive and 24 negative. All 42 had a positive NETest (100%). Twenty-one of the 24 had a negative NETest.  $^{68}\text{Ga}$ -SSA-PET/CT was performed in 34; 24 were positive and all 24 had a positive NETest. Eight of the ten who were negative by  $^{68}\text{Ga}$ -SSA-PET/CT also had a negative NETest. Dual modality (CT or MRI and  $^{68}\text{Ga}$ -SSA-PET/CT) was available in 33, 25 were image positive and all had an elevated NETest. Among eight INDs, seven had a negative NETest (Fig. 5 and Table 2).

#### SINETs

CT or MRI was performed in 44, 28 were positive and 16 negative. All 28 image positive had a positive NETest. Ten of the 16 image negative had a negative NETest.  $^{68}\text{Ga}$ -SSA-PET/CT was performed in 35; 32 were positive and the majority (31/32) had a positive NETest. Two of the three who were negative by imaging also had a negative NETest. Dual modality was available in 35, 32 were image positive and 31 had elevated NETest. Among three IND, two had a negative NETest.

Overall, the NETest was 92% (101/110) concordant with anatomical imaging (CT or MRI), 94% (65/69) concordant with  $^{68}\text{Ga}$ -SSA-PET/CT and 96% (65/68) concordant with dual modality imaging (CT/MRI and  $^{68}\text{Ga}$ -SSA-PET/CT) (Fig. 5 and Table 2). In image-positive CT/MRI ( $n=70$ ), NETest was elevated in all 70 ( $37 \pm 22$ ). In CT/MRI-negative ( $n=40$ ), NETest was normal ( $11 \pm 10$ ) in 31. In image-positive  $^{68}\text{Ga}$ -SSA-PET/CT ( $n=56$ ), the NETest was elevated ( $36 \pm 22$ ) in 55. In image-negative  $^{68}\text{Ga}$ -SSA-PET/CT ( $n=13$ ), the NETest was normal in 10 ( $9 \pm 8$ ).

There were six image-discordant results (all in WD NETs): five  $^{68}\text{Ga}$ -SSA-PET/CT positive/CT negative with NETest positive (Fig. 6) in four and one  $^{68}\text{Ga}$ -SSA-PET/CT-negative/CT-positive with NETest positive. Among dual modality positive ( $n=57$ ), 56 had elevated NETest. Nine of 11 INDs had a NETest within normal range ( $8 \pm 7$ ).

#### Disease status

Disease status assessed by RECIST 1.1: progressive disease ( $n=11$ ; PNET,  $n=8$ ; SINET,  $n=3$ ). Stable disease ( $n=64$ ; PNET:  $n=34$ ; SINET:  $n=30$ ). PD NETest levels were significantly ( $P < 0.0001$ ) higher ( $61 \pm 26$ ) than in stable disease (SD) ( $29 \pm 14$ ) (Fig. 7A). The majority (61/64) of NETs adjudged image stable (Fig. 7B) had a low NETest. Three exhibited a high score consistent with biochemical evidence of clinical disease activity or progression. Seven (7/11) individuals adjudged to be image progressive had a high score ( $79 \pm 10$ ). All seven were identified as having multiple, large ( $>10\text{mm}$ ) new lesions. In four with lower scores ( $44 \pm 6$ ), progression was considered to have occurred based upon the identification of a single new  $<10\text{mm}$  lesion over a median 12 months. The overall accuracy of the NETest for differentiating PD from SD based on a cut-off of NETest of 40 (23, 24, 26) was 95%.

#### Discussion

There has been considerable discussion about the need for an effective biomarker with clinical utility in NETs. Consensus statements have concluded that current monoanalyte biomarkers have diminished clinical utility (30). The previous default biomarker

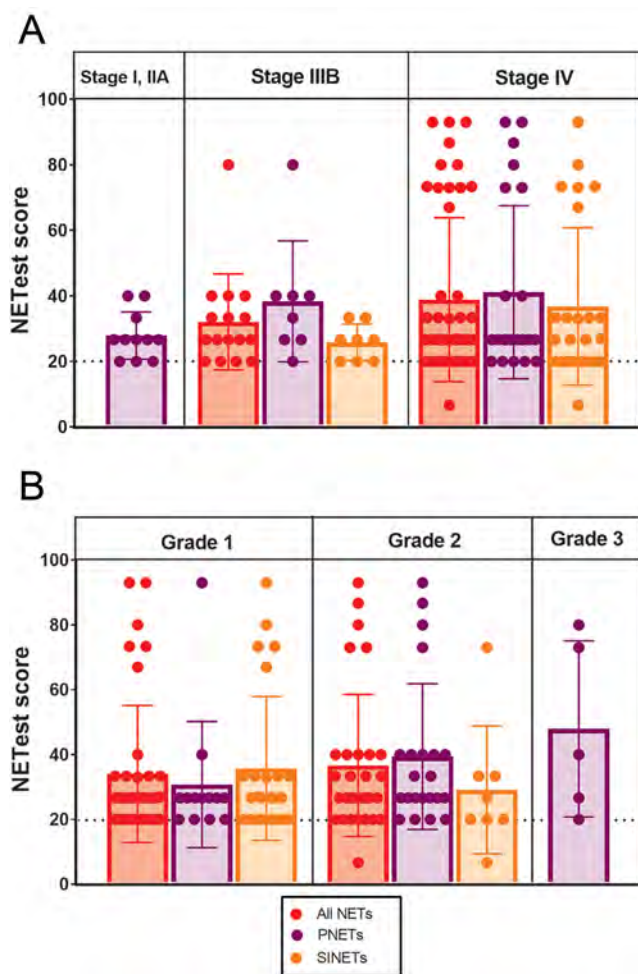


**Figure 4**

NETest levels in IPD according to TNM stage or grade. (A) NETest in IPD according to TNM stage (5, 36, 37): NETest levels were not significantly different between TNM stages; NETest in localized disease (PNETs: stage I and IIA,  $n = 11$ ) was  $28 \pm 7$ ; in stage III B NETs ( $n = 16$ ):  $32 \pm 15$ , PNETs ( $n = 8$ ):  $38 \pm 18$ , SINETs ( $n = 8$ ):  $26 \pm 6$ ; in stage IV NETs ( $n = 48$ ):  $39 \pm 25$ , PNETs ( $n = 23$ ):  $41 \pm 26$ , SINETs ( $n = 25$ ):  $37 \pm 24$  and were not significantly different. Two-tailed non-parametric tests (Mann-Whitney  $U$  test). Statistical significance was defined at a  $P$  value  $< 0.05$ . Mean  $\pm$  SD. (B) NETest in IPD according to grade: NETest levels were not significantly different between grades; NETest in G1: NETs ( $n = 38$ ):  $34 \pm 21$ , PNETs ( $n = 13$ ):  $31 \pm 19$ , SINETs ( $n = 25$ ):  $36 \pm 22$ ; in G2 NETs ( $n = 30$ ):  $37 \pm 21$ , PNETs ( $n = 22$ ):  $39 \pm 22$ , SINETs ( $n = 8$ ):  $29 \pm 20$ ; in G3 PNETs ( $n = 5$ ):  $48 \pm 27$  and were not significantly different. Two-tailed non-parametric tests (Mann-Whitney  $U$  test). Statistical significance was defined at a  $P$  value  $< 0.05$ . Mean  $\pm$  SD.

CgA is known to have limited if any clinical value in discriminant analysis studies (30). In the current study, the NETest was 97% accurate, 99% sensitive and 95% specific for a NET diagnosis. These metrics meet the NIH-proposed criteria of an optimal diagnostic biomarker (30) and are concordant with data from the previously reported GEP-NET studies. In a prospective study, NETest was 93% accurate in

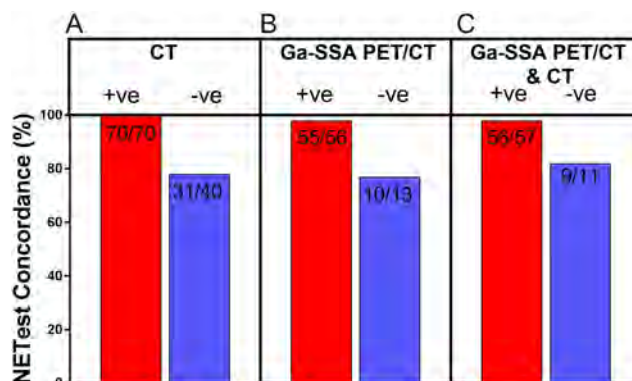


**Figure 5**

NETest concordance with imaging (morphologic and functional). Positive = red. Negative = blue. (A) Anatomical imaging was performed in 110 NETs (CT in 103, MRI in 4, CT and MRI in 3): 70 image positive, with NETest elevated in all; 40 image negative, with NETest normal in 31, and NETest elevated in 9: 4 were  $^{68}\text{Ga}$ -SSA-PET/CT positive; 3 had only single imaging modality performed (CT in 2, MRI in 1) and 2 were dual modality negative. (B)  $^{68}\text{Ga}$ -SSA-PET/CT was performed in 69:  $^{68}\text{Ga}$ -SSA-PET/CT was positive in 56, with NETest elevated in 55;  $^{68}\text{Ga}$ -SSA-PET/CT was negative in 13 with NETest normal in 10. (C) Dual modality imaging was performed in 68. Image positive ( $n = 57$ ), NETest was elevated in 56; 11 were dual image negative with NETest normal in 9.

identifying SINET and 94% for PNET diagnosis (31). In a large cohort ( $n = 140$  NETs,  $n = 113$  controls) from the Netherlands, the diagnostic accuracy was 93% (32). In a separate real-world study of 100 NET patients undertaken in US secondary and tertiary institutions, the diagnostic accuracy was confirmed as 97% in GEP-NETs (23).

To assess the NETest diagnostic efficacy, we compared its concordance with radiological evidence of the disease, since imaging is the critical arbiter in NET disease diagnostic work-up and monitoring (9). The concordance between a positive NETest score and imaging was high ( $> 90\%$ ). Specifically, it was 92% (101/110) with anatomical imaging, 94% (65/69) with functional imaging and 96% (65/68) when compared to two imaging modalities (either CT or MRI and  $^{68}\text{Ga}$ -SSA-PET/CT) were combined. In IPD, the NETest was 70/70 concordant with anatomical imaging, and it was 55/56 concordant with  $^{68}\text{Ga}$ -SSA-PET/CT. In one case, the NETest was normal and CT was negative, while  $^{68}\text{Ga}$ -SSA-PET/CT showed increased tracer uptake in three abdominal lymph nodes and focal uptake in the liver segment II. This patient developed liver metastases detectable by anatomical imaging (CT) 7 months later.

In the assessment of NETest concordance with image-negative NETs, there was a 'lower' concordance between the NETest and CT-negative results (31/40). This was, for the most part, due to false-negative CT results. In five cases

**Table 2** Summary of the NETest concordance with imaging performed in the entire NET cohort.

Imaging	Anatomical		Functional		Dual modality	
<b>PNETs (n = 67)</b>						
Examinations (no.)	66		34		33	
Modalities	CT: 62 MRI: 2 CT and MRI: 2		<sup>68</sup> Ga-SSA-PET/CT: 34		<sup>68</sup> Ga-SSA-PET/CT & CT: 31 <sup>68</sup> Ga-SSA-PET/CT and CT and MRI: 2	
Image positivity	+ve	-ve	+ve	-ve	+ve	-ve
Number	42	24	24	10	25	8
NETest +ve	42	3	24	2	25	1
NETest -ve	0	21	0	8	0	7
NETest concordance with imaging	42/42	21/24	24/24	8/10	25/25	7/8
<b>SINETs (n = 44)</b>						
Examinations (no.)	44		35		35	
Modalities	CT: 41 MRI: 2 CT and MRI: 1		<sup>68</sup> Ga-SSA-PET/CT: 35		<sup>68</sup> Ga-SSA-PET/CT & CT: 33 <sup>68</sup> Ga-SSA-PET/CT and MRI: 1 <sup>68</sup> Ga-SSA-PET/CT and CT and MRI: 1	
Image positivity	+ve	-ve	+ve	-ve	+ve	-ve
Number	28	16	32	3	32	3
NETest +ve	28	6	31	1	31	1
NETest -ve	0	10	1	2	1	2
NETest concordance with imaging	28/28	10/16	31/32	2/3	31/32	2/3
<b>All (PNETs and SINETs) (n = 111)</b>						
Examinations (no.)	110		69		68	
Modalities	CT: 103 MRI: 4 CT and MRI: 3		<sup>68</sup> Ga-SSA-PET/CT: 69		<sup>68</sup> Ga-SSA-PET/CT & CT: 64 <sup>68</sup> Ga-SSA-PET/CT and MRI: 1 <sup>68</sup> Ga-SSA-PET/CT and CT and MRI: 3	
Image positivity	+ve	-ve	+ve	-ve	+ve	-ve
Number	70	40	56	13	57	11
NETest +ve	70	9	55	3	56	2
NETest -ve	0	31	1	10	1	9
NETest concordance with imaging	70/70	31/40	55/56	10/13	56/57	9/11
Concordance Summary	Anatomical (101/110) 92%		Functional (65/69) 94%		Dual modality (65/68) 96%	

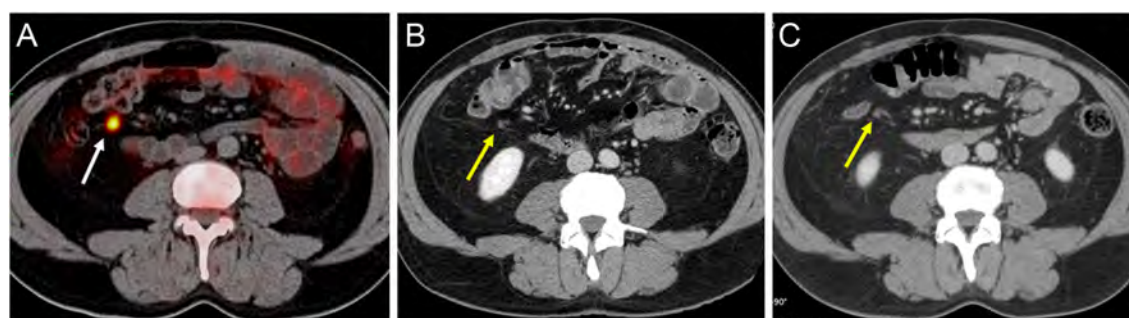


**Figure 6** Elevated NETest measurement correlates with <sup>68</sup>Ga-DOTA-TATE PE/CT in identifying metastatic disease, while CT remains negative. A patient diagnosed with SINET G1, 7 years post resection (p[m]T3N0M0, R0, LVI 0, Ki-67 1%) exhibited a positive NETest measurement (27%). (A) <sup>68</sup>Ga-DOTA-TATE PET/CT identified two tracer-avid subcentimeter mesenteric nodes/nodules (SUVmax 13.3 – white arrow and 8.7 – adjacent to the right aspect of the transverse colon). (B) Diagnostic abdominal CT was obtained which confirmed the absence of pathologically enlarged nodes/nodules at the site of the <sup>68</sup>Ga-SSA PET/CT uptake (yellow arrow). The patient subsequently developed abdominal pain and diarrhea and SSA therapy was initiated. (C) A follow-up diagnostic abdominal CT 16 months later again did not identify any pathologically enlarged node at this site (yellow arrow). LVI, lymphovascular invasion; R, resection margin; SSA, somatostatin analog.

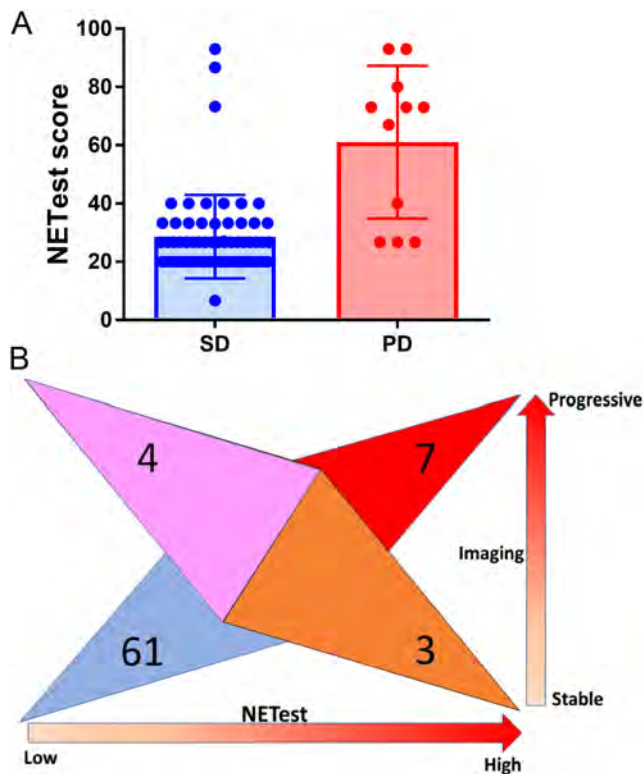


**Figure 7** NETest levels in stable and progressive disease. (A) NETest in stable vs progressive disease: NETest was significantly elevated in PD ( $n = 11$ ) ( $61 \pm 26$ ) compared to stable disease ( $n = 64$ ) ( $29 \pm 14$ ) ( $P < 0.0001$ ). Two-tailed non-parametric tests (Mann-Whitney  $U$  test). Statistical significance was defined at a  $P$  value  $< 0.05$ . Mean  $\pm$  SD. (B) Concordance of image- and NETest-based disease progression: The majority (95%) of patients ( $n = 61$ ) who were considered image stable (bottom left) had a low NETest. Three exhibited a high score consistent with biochemical evidence of disease progression. Sixty-four percent ( $n = 7$ ) of image-progression patients had a high score which correlated with the identification of multiple new large lesions at imaging. A further four patients had low scores; all of whom were identified with single, new small solitary lesion over a median 12-month follow-up.

with both CT and  $^{68}\text{Ga}$ -SSA-PET/CT imaging available, CT was negative but  $^{68}\text{Ga}$ -SSA-PET/CT identified lymph node metastases (in three), and in two others, lymph node as well as liver metastases were evident. In four, the NETest was positive. The NETest therefore identifies lesions that are not detected by CT.

Based on these observations as well as the known sensitivity discrepancy between morphologic and functional ( $^{68}\text{Ga}$ -SSA-PET/CT) imaging modalities, we considered a patient image negative when confirmed by two modalities (CT or MRI and  $^{68}\text{Ga}$ -SSA-PET/CT in WD NETs). A double image-negative status demonstrated a clearer indication of concordance between the NETest assay and those without disease. There were 11 NETs (8 PNETs, 3 SINETs) with dual modality imaging and no

radiological evidence of disease at blood draw. In two, the NETest was positive, but in each case, the results were borderline positive (20%). In one of these, a blood draw took place 5 months after distal pancreatectomy for stage I NF-PNET (resection margin-negative (R0); Ki-67 1%). In the other, a SINET, blood was collected 1 month after right hemicolectomy for an ileocecal valve NET (pT3N1, R0; Ki-67 1%); 12 months later, a follow-up CT was negative. It is likely in these two cases that the NETest was detecting microscopic disease.

Among 24 CT-negative or MRI-negative cases (in which  $^{68}\text{Ga}$ -SSA-PET/CT was not available at the time of blood draw), three cases had moderately elevated NETest: two PNETs (CT negative; NETest scores: 33% and 47%) and one SINET (MRI negative; NETest score: 27%). This was indicative of NET disease but with low biological activity. The first case (NF-PNET, Ki-67 4%; 15 months after distal pancreatectomy, pT4N0), at the time of a blood draw, had two hyper-vascular lesions (segment VIII) identified by CT. On a follow-up MRI, these were defined as perfusion disturbances; a  $^{68}\text{Ga}$ -SSA-PET/CT performed thereafter (within 4 months) revealed slightly increased tracer uptake in orbital bones, without any corresponding lesions on a CT, and with no pathological uptake in the liver – further radiological follow-up was recommended. Another case (NETest 47%), NF-PNET ~3.8 years after pancreaticoduodenectomy (Traverso, pT3N0, Ki-67  $< 2\%$ ), at the time of blood draw was CT negative (there were unsuspecting liver cysts). A follow-up  $^{68}\text{Ga}$ -SSA-PET/CT 3 months post blood draw was normal. The third case (SINET), ~5 years after right hemicolectomy for ileocecal valve NET (stage I, R0, Ki-67  $< 1\%$ ), was MRI negative at blood draw. Six months earlier, the  $^{68}\text{Ga}$ -SSA-PET/CT was negative. It is likely that these results represent the fact that elevations in NETest can precede alterations in imaging by (6–24 months). Previous reports have documented that elevations in the NETest are consistent with disease progression and are detectable in blood a significant time period before image alterations are evident (24, 26). For example, in a surgical series, those with microscopic disease (positive resection margins) and an elevated NETest (despite negative imaging at the time of blood draw) developed surgical recurrence within 6–12 months after R0 resection (25, 33).

There were six NET subjects in whom the morphologic and functional imaging results were discordant: five  $^{68}\text{Ga}$ -SSA-PET/CT positive and CT negative with NETest positive in four and one  $^{68}\text{Ga}$ -SSA-PET/CT negative but CT positive which was NETest positive. In cases where CT was negative, while  $^{68}\text{Ga}$ -SSA-PET/CT was positive,

the 'lower' concordance of the NETest with CT reflects 'false-negative' results in this imaging modality are consistent with the known increased efficacy of functional imaging (13, 15).  $^{68}\text{Ga}$ -SSA-PET/CT is considered more sensitive than CT in the detection of WD lesions (13), with Ki-67 <15%; however, in one patient, the CT was positive (single small liver lesion) and  $^{68}\text{Ga}$ -SSA-PET/CT was negative (a well-known limitation of SRS; Ki-67 3%).

Tumor heterogeneity has an impact on imaging sensitivity; therefore, it is apparent that no single imaging modality can be exclusively used to diagnose or detect the disease. Overall, combined imaging strategies are more effective, if available. However, follow-up with multiple imaging tools has risks (increased radiation exposure) and represents a high economic burden for the healthcare system. Moreover, resolution limitations (and the consequent difficulties with detection of meaningful size changes, especially in slow-growing or high-burden disease) result in the need for repetitive imaging, for example, every 3 months. Overall, imaging, especially when used to apply RECIST, has limitations. Thus, RECIST is inadequate for the early assessment of progression. This is a particular problem in NET disease, where the disease tends to grow slowly and, by definition, no progression is evident until the sum of the longest diameters has increased by 20%. In the case of volume, this therefore requires a substantial increase in tumor volume before it is defined as progression. Alternatively, for small-volume disease (2–3 mm), this 20% value cannot be easily identified and leads to incorrect attribution of progression in case of human-based measurement errors. The well-established RECIST 1.1 considers only a maximum of five lesions in total, maximum of two per organ. Certainly, in NET disease, where patients frequently present with extensive metastases, a sum of five lesions may well be non-representative of the entirety of the disease. In addition, bone disease is non-measurable, by definition, since the majority of bone metastases are (faintly) sclerotic and not lytic and frequently seen on  $^{68}\text{Ga}$ -DOTA-TATE PET/CT, rather than CT or MRI, which are the techniques considered in RECIST. RECIST 1.1 also includes PET (FDG-PET for solid tumors) to complement CT in the disease assessment. In NETs, FDG-PET is notoriously inefficient to detect the entirety of the disease and, to date,  $^{68}\text{Ga}$ -DOTATATE and/or a combination of FDG- and  $^{68}\text{Ga}$ -DOTA-TATE-PET/CT has not been incorporated in the response evaluation criteria. It has also been recognized that molecular imaging responses can also precede the morphologic response by several weeks (34).

Given the limitations of imaging, the use of an adjunctive strategy such as liquid biopsy may provide important information. Thus, a non-invasive liquid biopsy such as the NETest, which functions as an accurate diagnostic, and as noted in this study, correlates with imaging, is of likely clinical value.

It has been reported that the 'omic' cluster analysis which forms the basis of the multianalyte algorithm of the NETest are accurate in differentiating stable from progressive disease (35). In our cohort, 11 patients (8 PNET, 3 SINET) exhibited progressive and 64 stable disease. NETest levels were significantly elevated in PD ( $61 \pm 26$ ) compared to SD ( $29 \pm 14$ ). Using a cut-off of 40 (23, 24, 26), the NETest was 95% accurate in differentiating SD from PD. The identification of multiple, large (>10 mm) new lesions were associated with high scores ( $79 \pm 10$ ). Single, new smaller lesions were associated with lower scores ( $44 \pm 6$ ). Three patients of those considered SD (3/64) had NETest scores >40. In one, clinical evidence of disease progression was noted at the time of blood draw. In the second, a subsequent CT 6 months after blood draw confirmed progression (target lesions >20%). The third patient (NF-PNET, Ki67 8%) has previously undergone six cycles of PRRT. It is likely, given that imaging underestimates disease progression, that longer follow-up in this patient will demonstrate evidence of progression.

The majority of the image-positive cohort (54/75) was on SSA; therefore, the NETest can provide adjunctive information that supports the demonstration of therapeutic efficacy of SSA. The NETest utility in predicting SSA treatment response has already been reported in a separate NET cohort ( $n=28$ ) receiving SSAs (26). Multiple regression analysis in this cohort demonstrated that the NETest effectively predicted the onset of progressive disease while on SSA ( $p=0.0002$ ). Of more importance, NETest increased significantly earlier (~5 months prior) than imaging for RECIST-defined disease progression (treatment failure) in this cohort. The assay was considered effective in the identification of progressive disease (26).

This clinical utility of the NETest has been recently reported in a real-world study based upon an independent registry (23). This study demonstrated a very good concordance (83–88%) between the NETest with imaging, especially functional. It also provided useful preliminary information indicating that the NETest was effective in differentiating SD from progression and that it may be more sensitive in detecting progression before it is apparent on imaging. A prospective, large study is needed

to precisely define how effective the NETest alone is in identifying progression and how much earlier it can detect alterations in disease status.

It should be noted that the current study was based upon real-world principles. Therefore, although the entire study cohort comprised 174 subjects: 111 NET patients and 63 controls, the number of subjects in PNET and SINET subgroups was limited (reflecting a 12-month enrolment by one-center in a relatively rare disease). The follow-up period may have varied among the study subjects (median 8 months (1.5–24 months)). Furthermore, functional imaging was not available at blood draw in all (<sup>68</sup>Ga-SSA-PET/CT was available in 69 and FDG-PET/CT in 8), and there were only 11 progressive cases while imaging. Since only six subjects were high grade (three well- and three poorly differentiated), this did not allow a sub-analysis of the NETest efficacy in this more aggressive group of neuroendocrine neoplasia. Based upon these limitations, we would propose that further assessment of the relationship of NETest and imaging would require a future, larger and prospective study to extend the current results. Nevertheless, despite these limitations, the current data provide clear evidence that a blood-based multigene biomarker provides accurate information that is concordant with imaging. Use of the NETest information obtained by venipuncture may provide a point of care basis for monitoring disease, thereby decreasing the health costs of imaging and patient exposure to radiation.

## Conclusions

The NETest has been independently validated as an accurate diagnostic biomarker for SINET and PNET. These results are concordant with imaging and provide a good assessment of disease status. The NETest was as accurate as imaging as a diagnostic. The use of a multianalyte gene blood test and imaging may provide adjunctive information that can facilitate the management of NET disease.

### Declaration of interest

The authors declare that there is no conflict of interest that could be perceived as prejudicing the impartiality of the research reported.

### Funding

This work was supported by the Medical University of Silesia. Wren Laboratories provided sample measurement at no cost.

## References

- 1 Dasari A, Shen C, Halperin D, Zhao B, Zhou S, Xu Y, Shih T & Yao JC. Trends in the incidence, prevalence, and survival outcomes in patients With neuroendocrine tumors in the United States. *JAMA Oncology* 2017 **3** 1335–1342. (<https://doi.org/10.1001/jamaoncol.2017.0589>)
- 2 Pavel M, O'Toole D, Costa F, Capdevila J, Gross D, Kianmanesh R, Krenning E, Knigge U, Salazar R, Pape UF, *et al.* Enets consensus guidelines update for the management of distant metastatic disease of intestinal, pancreatic, bronchial neuroendocrine neoplasms (NEN) and NEN of unknown primary site. *Neuroendocrinology* 2016 **103** 172–185. (<https://doi.org/10.1159/000443171>)
- 3 Frilling A, Modlin IM, Kidd M, Russell C, Breitenstein S, Salem R, Kwekkeboom D, Lau WY, Klersy C, Vilgrain V, *et al.* Recommendations for management of patients with neuroendocrine liver metastases. *Lancet Oncology* 2014 **15** e8–e21. ([https://doi.org/10.1016/S1470-2045\(13\)70362-0](https://doi.org/10.1016/S1470-2045(13)70362-0))
- 4 Falconi M, Eriksson B, Kaltsas G, Bartsch DK, Capdevila J, Caplin M, Kos-Kudla B, Kwekkeboom D, Rindi G, Kloppel G, *et al.* Enets consensus guidelines update for the management of patients with functional pancreatic neuroendocrine tumors and non-functional pancreatic neuroendocrine tumors. *Neuroendocrinology* 2016 **103** 153–171. (<https://doi.org/10.1159/000443171>)
- 5 Kos-Kudla B, Rosiek V, Borowska M, Baldys-Waligorska A, Bednarczuk T, Blicharz-Dorniak J, Bolanowski M, Boratyn-Nowicka A, Cichocki A, Cwikla JB, *et al.* Pancreatic neuroendocrine neoplasms – management guidelines (recommended by the Polish Network of Neuroendocrine Tumours). *Endokrynologia Polska* 2017 **68** 169–197. (<https://doi.org/10.5603/EP.2017.2016>)
- 6 Srirajaskanthan R, Shanmugabavan D & Ramage JK. Carcinoid syndrome. *BMJ* 2010 **341** c3941. (<https://doi.org/10.1136/bmj.c3941>)
- 7 Ruf J, Schiefer J, Kropf S, Furth C, Ulrich G, Kosiek O, Denecke T, Pavel M, Pascher A, Wiedenmann B, *et al.* Quantification in (68) Ga-DOTA(0)-Phe(1)-Tyr(3)-octreotide positron emission tomography/computed tomography: can we be impartial about partial volume effects? *Neuroendocrinology* 2013 **97** 369–374. (<https://doi.org/10.1159/000350418>)
- 8 Virgolini I, Ambrosini V, Bomanji JB, Baum RP, Fanti S, Gabriel M, Papanthasiou ND, Pepe G, Oyen W, De Cristoforo C, *et al.* Procedure guidelines for PET/CT tumour imaging with <sup>68</sup>Ga-DOTA-conjugated peptides: <sup>68</sup>Ga-DOTA-TOC, <sup>68</sup>Ga-DOTA-NOC, <sup>68</sup>Ga-DOTA-TATE. *European Journal of Nuclear Medicine and Molecular Imaging* 2010 **37** 2004–2010. (<https://doi.org/10.1007/s00259-010-1512-3>)
- 9 Oberg K, Krenning E, Sundin A, Bodei L, Kidd M, Tesselar M, Ambrosini V, Baum RP, Kulke M, Pavel M, *et al.* A Delphic consensus assessment: imaging and biomarkers in gastroenteropancreatic neuroendocrine tumor disease management. *Endocrine Connections* 2016 **5** 174–187. (<https://doi.org/10.1530/EC-16-0043>)
- 10 Kidd M, Bodei L & Modlin IM. Chromogranin A: any relevance in neuroendocrine tumors? *Current Opinion in Endocrinology, Diabetes, and Obesity* 2016 **23** 28–37. (<https://doi.org/10.1097/MED.000000000000215>)
- 11 de Mestier L, Dromain C, d'Assignies G, Scoazec JY, Lassau N, Lebtahi R, Brixi H, Mitry E, Guimbaud R, Courbon F, *et al.* Evaluating digestive neuroendocrine tumor progression and therapeutic responses in the era of targeted therapies: state of the art. *Endocrine-Related Cancer* 2014 **21** R105–R120. (<https://doi.org/10.1530/ERC-13-0365>)
- 12 Schwartz LH, Litière S, de Vries E, Ford R, Gwyther S, Mandrekar S, Shankar L, Bogaerts J, Chen A, Dancey J, *et al.* RECIST 1.1-update and clarification: from the RECIST committee. *European Journal of Cancer* 2016 **62** 132–137. (<https://doi.org/10.1016/j.ejca.2016.03.081>)
- 13 Bodei L, Sundin A, Kidd M, Prasad V & Modlin IM. The status of neuroendocrine tumor imaging: from darkness

- to light? *Neuroendocrinology* 2015 **101** 1–17. (<https://doi.org/10.1159/000367850>)
- 14 Choi H, Charnsangavej C, Faria SC, Macapinlac HA, Burgess MA, Patel SR, Chen LL, Podoloff DA & Benjamin RS. Correlation of computed tomography and positron emission tomography in patients with metastatic gastrointestinal stromal tumor treated at a single institution with imatinib mesylate: proposal of new computed tomography response criteria. *Journal of Clinical Oncology* 2007 **25** 1753–1759. (<https://doi.org/10.1200/JCO.2006.07.3049>)
  - 15 Toumpanakis C, Kim MK, Rinke A, Bergestuen DS, Thirlwell C, Khan MS, Salazar R & Oberg K. Combination of cross-sectional and molecular imaging studies in the localization of gastroenteropancreatic neuroendocrine tumors. *Neuroendocrinology* 2014 **99** 63–74. (<https://doi.org/10.1159/000358727>)
  - 16 Gibson WE, Gonzalez RS, Cates JMM, Liu E & Shi C. Hepatic micrometastases are associated with poor prognosis in patients with liver metastases from neuroendocrine tumors of the digestive tract. *Human Pathology* 2018 **79** 109–115. (<https://doi.org/10.1016/j.humpath.2018.05.006>)
  - 17 Malczewska A, Bodei L, Kidd M & Modlin IM. Blood mRNA measurement (NETest) for neuroendocrine tumors diagnosis of image-negative liver metastatic disease. *Journal of Clinical Endocrinology and Metabolism* 2019 **104** 867–872. (<https://doi.org/10.1210/jc.2018-01804>)
  - 18 Niederle B, Pape UF, Costa F, Gross D, Kelestimur F, Knigge U, Oberg K, Pavel M, Perren A, Toumpanakis C, *et al.* Enets consensus guidelines update for neuroendocrine neoplasms of the jejunum and ileum. *Neuroendocrinology* 2016 **103** 125–138. (<https://doi.org/10.1159/000443170>)
  - 19 Bodei L, Kidd MS, Singh A, van der Zwan WA, Severi S, Drozdov IA, Cwikla J, Baum RP, Kwekkeboom DJ, Paganelli G, *et al.* PRRT genomic signature in blood for prediction of (177)Lu-octreotate efficacy. *European Journal of Nuclear Medicine and Molecular Imaging* 2018 **45** 1155–1169. (<https://doi.org/10.1007/s00259-018-3967-6>)
  - 20 Siravegna G, Marsoni S, Siena S & Bardelli A. Integrating liquid biopsies into the management of cancer. *Nature Reviews Clinical Oncology* 2017 **14** 531–548. (<https://doi.org/10.1038/nrclinonc.2017.14>)
  - 21 Modlin IM, Drozdov I & Kidd M. The identification of gut neuroendocrine tumor disease by multiple synchronous transcript analysis in blood. *PLoS ONE* 2013 **8** e63364. (<https://doi.org/10.1371/journal.pone.0063364>)
  - 22 Modlin IM, Kidd M, Malczewska A, Drozdov I, Bodei L, Matar S & Chung KM. The NETest: the clinical utility of multigene blood analysis in the diagnosis and management of neuroendocrine tumors. *Endocrinology and Metabolism Clinics of North America* 2018 **47** 485–504. (<https://doi.org/10.1016/j.ecl.2018.05.002>)
  - 23 Liu E, Paulson S, Gulati A, Freudman J, Grosh W, Kafer S, Wickremesinghe PC, Salem RR & Bodei L. Assessment of NETest clinical utility in a U.S. Registry-based study. *Oncologist* 2018 **23** 1. (<https://doi.org/10.1634/theoncologist.2017-0623>)
  - 24 Pavel M, Jann H, Prasad V, Drozdov I, Modlin IM & Kidd M. NET blood transcript analysis defines the crossing of the clinical Rubicon: when stable disease becomes progressive. *Neuroendocrinology* 2017 **104** 170–182. (<https://doi.org/10.1159/000446025>)
  - 25 Filosso PL, Kidd M, Roffinella M, Lewczuk A, Chung KM, Kolasinska-Cwikla A, Cwikla J, Lowczak A, Doboszynska A, Malczewska A, *et al.* The utility of blood neuroendocrine gene transcript measurement in the diagnosis of bronchopulmonary neuroendocrine tumours and as a tool to evaluate surgical resection and disease progression. *European Journal of Cardio-Thoracic Surgery* 2018 **53** 631–639. (<https://doi.org/10.1093/ejcts/ezx386>)
  - 26 Cwikla JB, Bodei L, Kolasinska-Cwikla A, Sankowski A, Modlin IM & Kidd M. Circulating transcript analysis (NETest) in GEP-NETs treated With somatostatin analogs defines therapy. *Journal of Clinical Endocrinology and Metabolism* 2015 **100** E1437–E1445. (<https://doi.org/10.1210/jc.2015-2792>)
  - 27 Modlin IM, Aslanian H, Bodei L, Drozdov I & Kidd M. A PCR blood test outperforms chromogranin A in carcinoid detection and is unaffected by proton pump inhibitors. *Endocrine Connections* 2014 **3** 215–223. (<https://doi.org/10.1530/EC-14-0100>)
  - 28 Zweig MH & Campbell G. Receiver-operating characteristic (ROC) plots: a fundamental evaluation tool in clinical medicine. *Clinical Chemistry* 1993 **39** 561–577.
  - 29 Hanley JA & McNeil BJ. A method of comparing the areas under receiver operating characteristic curves derived from the same cases. *Radiology* 1983 **148** 839–843. (<https://doi.org/10.1148/radiology.148.3.6878708>)
  - 30 Oberg K, Modlin IM, De Herder W, Pavel M, Klimstra D, Frilling A, Metz DC, Heaney A, Kwekkeboom D, Strosberg J, *et al.* Consensus on biomarkers for neuroendocrine tumour disease. *Lancet Oncology* 2015 **16** e435–e446. ([https://doi.org/10.1016/S1470-2045\(15\)00186-2](https://doi.org/10.1016/S1470-2045(15)00186-2))
  - 31 Modlin IM, Kidd M, Bodei L, Drozdov I & Aslanian H. The clinical utility of a novel blood-based multi-transcriptome assay for the diagnosis of neuroendocrine tumors of the gastrointestinal tract. *American Journal of Gastroenterology* 2015 **110** 1223–1232. (<https://doi.org/10.1038/ajg.2015.160>)
  - 32 van Treijen MJC, Korse CM, van Leeuwen RS, Saveur LJ, Vriens MR, Verbeek WHM, Tesselar MET & Valk GD. Blood transcript profiling for the detection of neuroendocrine tumors: results of a large independent validation study. *Frontiers in Endocrinology* 2018 **9** 740. (<https://doi.org/10.3389/fendo.2018.00740>)
  - 33 Modlin IM, Frilling A, Salem RR, Alaïmo D, Drymoussis P, Wasan HS, Callahan S, Faiz O, Weng L, Teixeira N, *et al.* Blood measurement of neuroendocrine gene transcripts defines the effectiveness of operative resection and ablation strategies. *Surgery* 2016 **159** 336–347. (<https://doi.org/10.1016/j.surg.2015.06.056>)
  - 34 Haug AR, Auernhammer CJ, Wangler B, Schmidt GP, Uebles C, Goke B, Cumming P, Bartenstein P, Tiling R & Hacker M. 68Ga-DOTATATE PET/CT for the early prediction of response to somatostatin receptor-mediated radionuclide therapy in patients with well-differentiated neuroendocrine tumors. *Journal of Nuclear Medicine* 2010 **51** 1349–1356. (<https://doi.org/10.2967/jnumed.110.075002>)
  - 35 Kidd M, Drozdov I & Modlin I. Blood and tissue neuroendocrine tumor gene cluster analysis correlate, define hallmarks and predict disease status. *Endocrine-Related Cancer* 2015 **22** 561–575. (<https://doi.org/10.1530/ERC-15-0092>)
  - 36 Bednarczuk T, Bolanowski M, Zemczak A, Baldys-Waligorska A, Blicharz-Dorniak J, Boratyn-Nowicka A, Borowska M, Cichoński A, Cwikla JB, Falconi M, *et al.* Neuroendocrine neoplasms of the small intestine and appendix – management guidelines (recommended by the Polish Network of Neuroendocrine Tumours). *Endokrynologia Polska* 2017 **68** 223–236. (<https://doi.org/10.5603/EP.2017.0018>)
  - 37 Brierley JD, Gospodarowicz MK & Wittekind Ch (eds). *International Union Against Cancer (UICC). TNM Classification of Malignant Tumours*, 8th ed. Oxford, UK: John Wiley & Sons, 2017.

Received in final form 28 February 2019

Accepted 13 March 2019

Accepted Preprint published online 13 March 2019